ACCOUNTS
of chemical research

Unique Properties of Ceria Nanoparticles Supported on Metals: Novel Inverse Ceria/Copper Catalysts for CO Oxidation and the Water-Gas Shift Reaction

SANJAYA D. SENANAYAKE, DARIO STACCHIOLA, AND JOSE A. RODRIGUEZ*

Chemistry Department, Brookhaven National Laboratory, Upton, New York 11789, United States

RECEIVED ON JULY 31, 2012

CONSPECTUS

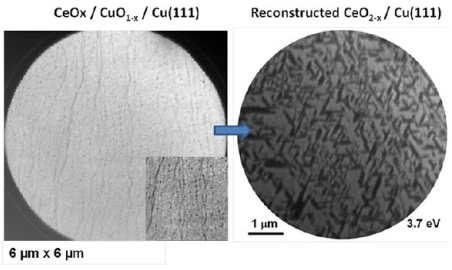

Oxides play a central role in important industrial processes, including applications such as the production of renewable energy, remediation of environmental pollutants, and the synthesis of fine chemicals. They were originally used as catalyst supports and were thought to be chemically inert, but now they are used to build catalysts tailored toward improved selectivity and activity in chemical reactions. Many studies have compared the morphological, electronic, and chemical properties of oxide materials with those of unoxidized metals. Researchers know much less about the properties of oxides at the nanoscale, which display distinct behavior from their bulk counterparts. More is known about metal nanoparticles.

Inverse-model catalysts, composed of oxide nanoparticles supported on metal or oxide substrates instead of the reverse (oxides supporting metal nanoparticles), are excellent tools for systematically testing the properties of novel catalytic oxide materials. Inverse models are prepared in situ and can be studied with a variety of surface science tools (e.g. scanning tunneling microscopy, X-ray photoemission spectroscopy, ultraviolet photoemission spectroscopy, low-energy electron microscopy) and theoretical tools (e.g. density functional theory). Meanwhile, their catalytic activity can be tested simultaneously in a reactor. This approach makes it possible to identify specific functions or structures that affect catalyst performance or reaction selectivity. Insights gained from these tests help to tailor powder systems, with the primary objective of rational design (experimental and theoretical) of catalysts for specific chemical reactions.

This Account describes the properties of inverse catalysts composed of CeO_x nanoparticles supported on Cu(111) or CuO_x/Cu(111) as determined through the methods described above. Ceria is an important material for redox chemistry because of its interchangeable oxidation states (Ce^{4+} and Ce^{3+}). Cu(111), meanwhile, is a standard catalyst for reactions such as CO oxidation and the water-gas shift (WGS). This metal serves as an ideal replacement for other noble metals that are neither abundant nor cost effective. To prepare the inverse system we deposited nanoparticles (2−20 nm) of cerium oxide onto the Cu(111) surface. During this process, the Cu(111) surface grows an oxide layer that is characteristic of Cu_2O (Cu^{1+}). This oxide can influence the growth of ceria nanoparticles. Evidence suggests triangular-shaped CeO_2(111) grows on Cu_2O(111) surfaces while rectangular CeO_2(100) grows on Cu_4O_3(111) surfaces.

We used the CeO_x/Cu_2O/Cu(111) inverse system to study two catalytic processes: the WGS ($CO + H_2O \rightarrow CO_2 + H_2$) and CO oxidation ($2CO + O_2 \rightarrow 2CO_2$). We discovered that the addition of small amounts of ceria nanoparticles can activate the Cu(111) surface and achieve remarkable enhancement of catalytic activity in the investigated reactions. In the case of the WGS, the CeO_x nanoparticle facilitated this process by acting at the interface with Cu to dissociate water. In the CO oxidation case, an enhancement in the dissociation of O_2 by the nanoparticles was a key factor.

The strong interaction between CeO_x nanoparticles and Cu(111) when preoxidized and reduced in CO resulted in a massive surface reconstruction of the copper substrate with the introduction of microterraces that covered 25−35% of the surface. This constitutes a new mechanism for surface reconstruction not observed before. These microterraces helped to facilitate a further enhancement of activity towards the WGS by opening an additional channel for the dissociation of water.

In summary, inverse catalysts of CeO_x/Cu(111) and CeO_2/Cu_2O/Cu(111) demonstrate the versatility of a model system to obtain insightful knowledge of catalytic processes. These systems will continue to offer a unique opportunity to probe key catalytic components and elucidate the relationship between structure and reactivity of novel materials and reactions in the future.

Published on the Web 01/03/2013 www.pubs.acs.org/accounts
10.1021/ar300231p

1. Introduction

Oxides have come to play a central role in important industrial processes, and in many instances are the *"sine qua non"* involved in chemical applications including the production of renewable energy, remediation of environmental pollutants, and the synthesis of fine chemicals.[1] In catalysis, the role of oxides has evolved over time, with their original use as simple supports that were thought to be chemically inert, to being used today exclusively in the engineering of catalysts with distinct architecture and composition tailored toward achieving optimum selectivity and activity in chemical reactions.[2] Fundamental studies using surface science tools and theoretical modeling (DFT) have provided an understanding of oxide chemistry through careful and systematic experimentation/modeling to yield unique insights into the distinct morphological, electronic, and chemical properties of oxide materials that are readily discerned from the properties of metals without oxygen.[3] These studies often related the structure of catalysts to the chemical reactivity and have been strikingly advantageous in the rational design of novel materials and understanding of chemical reaction pathways. Furthermore, the unique chemistry of nanomaterials have been exploited in numerous chemical reactions, but the phenomenological properties of oxide nanoparticles are understood to a far lesser extent than that of metal nanomaterials.[4]

Inverse oxide/metal catalysts provide a unique bench mark to understand the role of oxide nanoparticles in catalytic processes when combined with the fundamental tools of surface science and density-functional theory (DFT) calculations.[5−10] The *inverse model catalyst* system is a variant of the more traditional *supported model catalysts* with the distinction that oxide nanoparticles are dispersed on a metal surface as opposed to the use of the oxide as a support to disperse small nanoparticles of metals (Figure 1). The oxide growth can be easily varied from small clusters and nanoparticles that are a few nanometers (2−20 nm, coverage <1 ML) in size to larger three-dimensional (3-D) microparticles (50−300 nm, 1−5 ML) and can even be extended to ultrathin films (thickness $\sim$ 1−30 ML) to make comparisons to the bulk chemistry of the oxide. The electronic and chemical properties of the oxide particles can vary as a function of particle size and due to interactions with the support. The metal surface can be in the form of nonoxidizable metals such as Au(111)[5,6] or readily oxidizable metals such as Cu(111),[11] which is the focus of this Account.

The degree of oxidation occurring on the support metal has a great influence not only on the growth mode of the oxide nanoparticle but also on the chemistry associated with the subsequent reaction under investigation. Movement and spilling over of chemical reactants and redox agents (O, CO, H_2, H_2O, etc.) can occur between the oxide nanoparticle and the support with an interchange of redox properties between them. In addition, the *interface* of the oxide nanoparticle and the metal support can be a critical player associated with the main reaction pathway.[11]

In this Account, we will describe recent, systematic studies for CeO_x/Cu(111) and CeO_2/Cu_2O/Cu(111) model catalysts that illustrate the unique catalytic properties of ceria nanoparticles when present in ceria/metal or ceria/oxide interfaces. We are particularly interested in the ceria−copper oxide system because it has been characterized using a large array of techniques and can be taken all the way from model surfaces to high-surface area powder catalysts.[12,13] The next section discusses experimental and theoretical studies that deal with the intrinsic properties of nonsupported ceria nanoparticles. Then, we will examine the growth mode of ceria nanoparticles on well-defined surfaces of copper/copper oxide. This will be followed by a discussion of the phenomena responsible for the high catalytic activity of CeO_x/Cu(111) and CeO_2/Cu_2O/Cu(111) for the water-gas shift (WGS, $CO + H_2O \rightarrow CO_2 + H_2$) and CO oxidation ($CO + O_2 \rightarrow CO_2$) reactions. The last section of the Account focuses on nanopatterning in CeO_x/Cu(111) induced by the supported ceria nanoparticles and a new mechanism for surface reconstruction and enhancement of catalytic activity.

2. Intrinsic Properties of Ceria Nanoparticles

In the area of catalysis, nanoparticles of ceria have been studied since the early 1970s, but they were poorly characterized.[14,15] In recent years, substantial progress has been made thanks to the use of better synthesis methods and sophisticated techniques for characterizing structural and electronic properties.[4,15−17]

Images of high-resolution transmission electron microscopy (HRTEM) for well-prepared ceria nanoparticles indicate that in the size range of 3−10 nm the particles are crystalline and their shape predominantly corresponds to truncated octahedra defined by {111} and {100} facets; see Figure 2.[17] Classical molecular dynamics simulations[18] strongly suggest that the octahedral shape of such nanoparticles is inherent to this size of ceria nanoparticles. Neither in the atomistic models nor in the experiment were {110} facets detected in significant concentration, in spite of

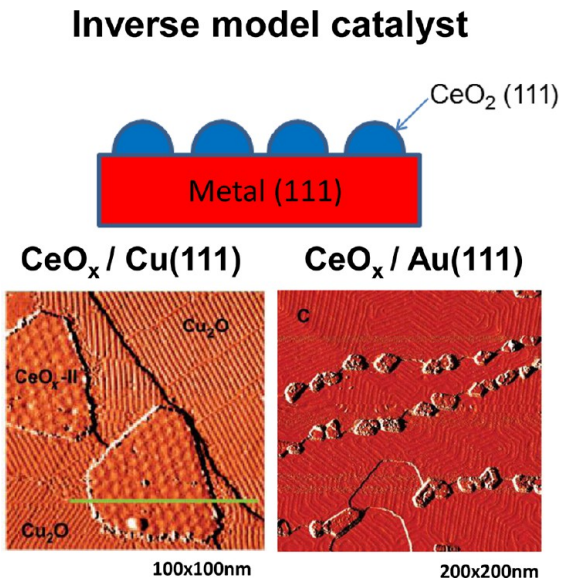

FIGURE 1. Top: Schematic of an inverse model catalyst. Bottom: Images of scanning tunneling microscopy for inverse CeOx/Cu_2O/Cu(111) and CeO_x/Au(111) model catalysts.

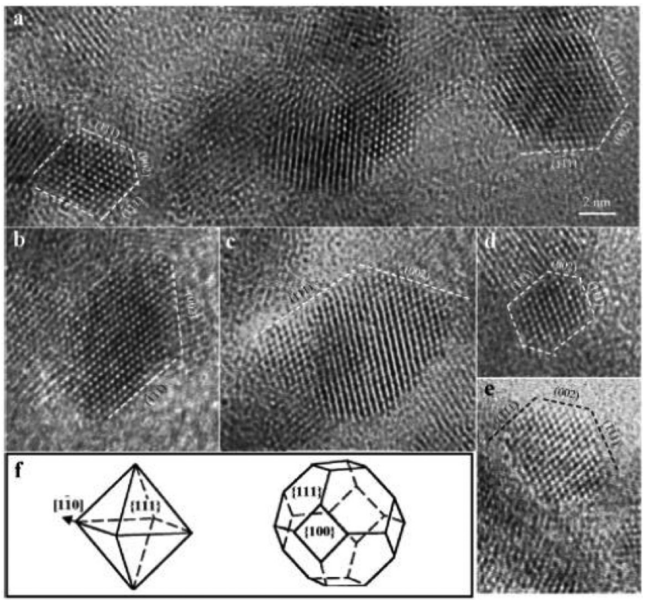

FIGURE 2. High resolution TEM of CeO_2 nanoparticles showing facet structures. Reprinted with permission from ref 17. Copyright 2003 American Chemical Society.

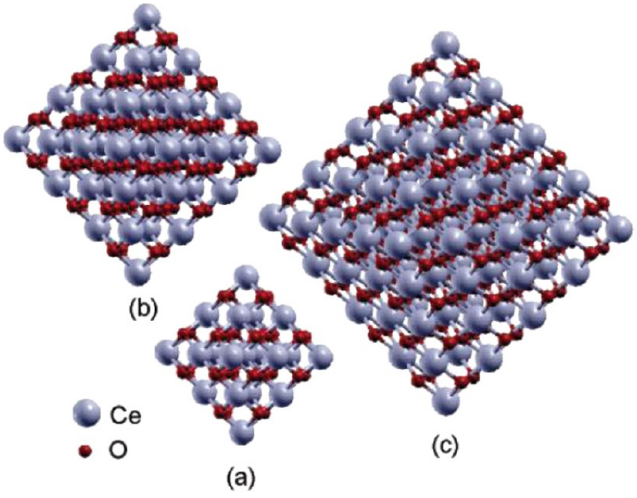

FIGURE 3. Octahedral Ceria nanoparticles cut in (111) from bulk CeO_2 including (a) $Ce_{19}O_{32}$, (b) $Ce_{44}O_{80}$, and (c) $Ce_{85}O_{160}$.[21,23] Reprinted with permission from ref 21. Copyright 2007 American Chemical Society.

the higher stability of the (110) surface compared to the (100) surface in bulk ceria. Employing a bottom-up approach, the structure and energetics of stoichiometric ceria clusters Ce_nO_{2n} ($n = 2-20$ and $n = 50$) were investigated using simulated annealing and interionic potentials.[19] The lattice energy decreased with increasing n. Only for the largest nanoparticles was the fluorite structure of bulk ceria clearly observed. Small nanoparticles exhibited a nearly amorphous structure. It is important to note that there is direct experimental evidence that the reducibility of Ceria has a dependency on its crystallinity.[20] In general, the energy required to reduce the Ce_nO_{2n} systems increased with particle size, but large fluctuations were also observed. The reduction of the ceria nanoparticles was structure sensitive, being easier in systems with a low degree of crystallinity. In general, this prediction has been verified in the case of ceria nanoparticles dispersed on metal surfaces,[5,9,11,13] as we will see below.

Recently DFT-based calculations were used to study a series of ceria nanoparticles $(CeO_{2-x})_m$ with $m \leq 85$.[21−23] The main focus of these studies was on the perfectly octahedral and truncated (cub-) octahedral particles which were obtained by cutting a particle from bulk ceria via the (111) and (100) crystallographic planes (see Figure 3). An important finding of these studies was that partially reduced Ce^{3+} cations tend to occupy low-coordinated surface positions whereas Ce^{4+} cations strongly prefer to reside at highly coordinated positions. Thus, Ce^{3+} species in nonstoichiometric ceria particles are expected to strongly affect the surface reactivity. The binding energies of the clusters $Ce_{19}O_{32}$, $Ce_{44}O_{80}$, and $Ce_{85}O_{160}$ converged to the bulk limit almost linearly with respect to the average coordination number of Ce.

The theoretical calculations predict that the existence of O vacancies and edge atoms in the ceria nanoparticles drastically affects their reactivity toward molecules such as CO, CO_2, O_2, and water, which are involved in CO oxidation and the water-gas shift reaction.[22,24]

3. Growth Mode of Ceria Nanoparticles on Metal Surfaces: Preparation of Inverse Oxide/Metal Catalysts

Preparation of inverse model catalysts usually takes place in situ and in ultrahigh vacuum chambers so as to minimize the exposure of ambient contaminants prior to experimentation. Cerium metal is vaporized at very high temperatures using a commercial electron beam metal evaporator and then deposited in an O_2 environment ($1-5 \times 10^{-7}$ Torr) onto a heated (~600 K) metal substrate [Cu(111)]. This process allows the cerium particles to be oxidized when approaching and upon first contact with the metal surface (Figure 4).

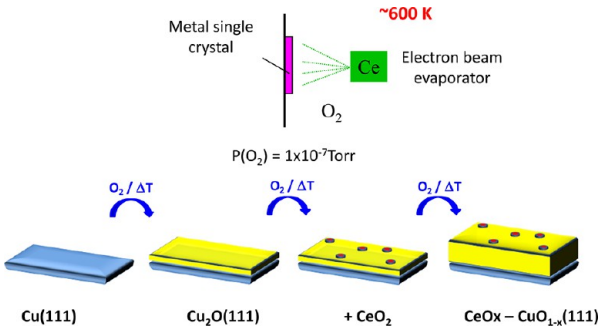

FIGURE 4. Schematic of evaporation process (top). Growth of CeO_x on a Cu(111) surface (bottom).

The Cu metal substrate when at elevated temperatures and in an oxygen ambient will start to grow a thin oxide layer (Cu_2O) prior to the deposition of the ceria nanoparticles. This oxidation process can be viewed in real time using low-energy electron microscopy (LEEM) (Figure 5) in the form of waves that cross the Cu terraces starting at step edges and ultimately coalesce into a thin oxide film.[25] Scanning tunneling microscopy (STM)[26] and low-energy electron diffraction (LEED) show that the surface is composed of a "44" reconstruction of Cu_2O[27] that is approached via several defected oxide structures composed of pentagons and hexagons termed a 5–7 structure of Cu_2O.[26]

The ceria nanoparticles grown on Cu(111) can have a range of size distributions (1–30 nm) and are (111) oriented on the surface exhibiting triangular shapes (Figure 6, left side) and showing a preference to nucleate at step edges. Growth temperature can influence the size of the particles, with smaller particles forming at lower temperatures while higher temperatures favor larger particles. Continued oxidation of the inverse systems shows the spillover of oxygen from ceria to copper in STM, and it is possible to observe the mechanism through which Cu oxidizes.[28] Deeper preoxidation of the Cu surface also can affect the growth of the Ceria particles with rectangular and (100) oriented particles observed when Cu(111) is preoxidized heavily with NO_2 to

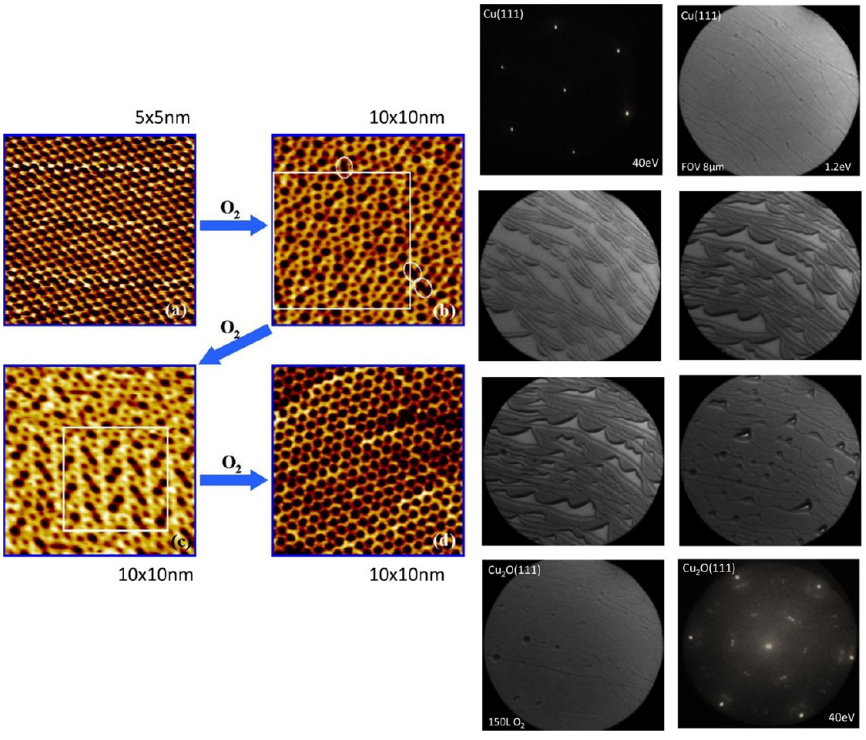

FIGURE 5. STM: Cu(111) oxidation to Cu_2O via a 5–7 defected structure to the "44" reconstructed $Cu_2O(111)$ at a total of 200L of O_2 (left).[25] LEEM: Real time oxidation of Cu(111) with the resulting "44" reconstruction of $Cu_2O(111)$ (right).[26]

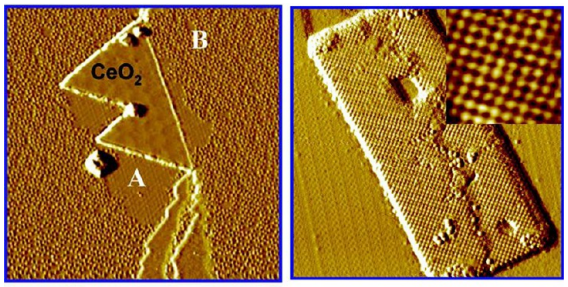

FIGURE 6. STM: (Left) STM of triangular CeO_2 nanoparticles oriented in (111) with oxygen spillover on Cu_2O substrate. (Right) STM of rectangular CeO_2 nanoparticles oriented in (100) on Cu_4O_3. Reprinted with permission from ref 29. Copyright 2011 American Chemical Society.

form Cu_4O_3.[29] The shape and morphology of the supported ceria nanoparticles is determined by strong interactions with the metal or oxide substrate, and one can find structures not seen in the case of nonsupported ceria nanoparticles.

In the literature, studies have been published for the deposition of ceria nanoparticles or films on close packed metal surfaces of Ni,[30] Cu,[31] Rh,[32] Ru,[33,34] Pd,[35] Re,[36] Pt,[37,38] and Au.[5] Well-ordered films were characterized at the atomic scale with STM in the cases of Cu(111), Ru(0 0 0 1), Rh(1 1 1), Pt(111), and Au(111). In principle, all of these systems can be used as inverse oxide/metal catalysts if one reduces the ceria coverage to sub-monolayer amounts generating only nanoparticles of this oxide. In the next section, we will describe studies that illustrate the special catalytic properties of ceria nanoparticles supported on Cu(111) and Cu_2O/Cu(111).

4. Fundamental Studies of Catalytic Reactions

To date the inverse model CeO_2/Cu_2O/Cu(111) catalyst shown in Figure 6 has been used to study two common reactions: the water-gas shift and CO oxidation.[11,28] On plain Cu(111), these reactions have been studied extensively both experimentally[39,40] and theoretically.[41,42] Bulk CeO_2 yields no activity toward either of these reactions, but the addition of a small amount of ceria nanoparticles to Cu(111) remarkably improves catalytic activity by several orders of magnitude, offering a new approach to activate copper surfaces.[11,28] The inverse CeO_x/Cu_2O/Cu(111) system has been studied with a cross section of tools including experiments with STM to understand surface structural modifications; reflection absorption infrared spectroscopy (RAIRS), X-ray photoemission spectroscopy (XPS) and near edge X-ray absorption fine structure (NEXAFS) to identify surface intermediates and chemical state of the surface; ambient pressure XPS to study the catalyst under reaction conditions and activity testing in a microreactor to determine performance.[11,28] Theoretical modeling using advanced DFT techniques was also used to elucidate likely mechanistic pathways and the stability of reaction intermediates. In the following section, we take a more specific look at both the WGS and CO oxidation reactions over CeO_2/Cu_2O/Cu(111) and CeO_x/Cu(111) surfaces.

a. Water Gas Shift Reaction. The water-gas shift reaction offers the ability to deliver clean H_2 to many technological applications.[43] This reaction is undertaken in the industry either using FeO_x/CrO_x based catalysts for high-temperature (573−773 K) processes or Cu based catalysts for low temperature (<520 K) processes.[43] For the two reaction mechanisms commonly proposed for this reaction (redox and carboxyl/associative), the most critical step (or the rate limiting step) is associated with the dissociation of H_2O to give OH.[41]

TABLE

associative mechanism	redox mechanism
CO (g) → CO (a)	CO (g) → CO (a)
H_2O (g) → H_2O (a)	H_2O (g) → H_2O (a)
H_2O (a) → OH (a) + H (a)	H_2O (a) → OH (a) + H (a)
CO (a) + OH (a) → COOH (a)	OH (a) → O (a) + H (a)
COOH (a) → CO_2 (g) + H (a)	OH (a) + OH (a) → H_2O (a) + O (a)
COOH (a) + OH (a) → CO_2 (a) + H_2O (a)	CO (a) + O (a) → CO_2 (a)
CO_2 (a) → CO_2 (g)	CO_2 (a) → CO_2 (g)
H (a) + H (a) → H_2 (g)	H (a) + H (a) → H_2

Under WGS reaction conditions, the CeO_2/Cu_2O/Cu(111) system seen in Figure 1 or 6 transforms into CeO_x/Cu(111).[11] Cu(111) has a steep activation barrier to overcome for dissociating H_2O (E_a = 0.9−1.4 eV). This barrier is considerably lowered in the presence of ceria nanoparticles, making the dissociation of H_2O more energetically favorable for the inverse catalyst.[11] This manifests in a considerably improved activity for the production of H_2 as depicted in Figure 7, where the CeO_x/Cu(111) catalysts is compared to other Cu based systems.

From this Arrhenius plot, we can learn that Cu(111) is the least active catalyst and it is clear from a comparison with a markedly improved Cu(100) that the reaction is structure sensitive.[39,44] If the Cu is in the form of nanoparticles and then supported on CeO_2(111), as a conventional supported model catalyst (Cu/CeO_2(111)), there is a further improvement in activity on account of the Cu nanoparticles that become activated on CeO_2(111). This system opens an interface between the Cu nanoparticles and the bulk cerium oxide. However, the inverse catalyst is considerably better than all the other models showing that the properties of the

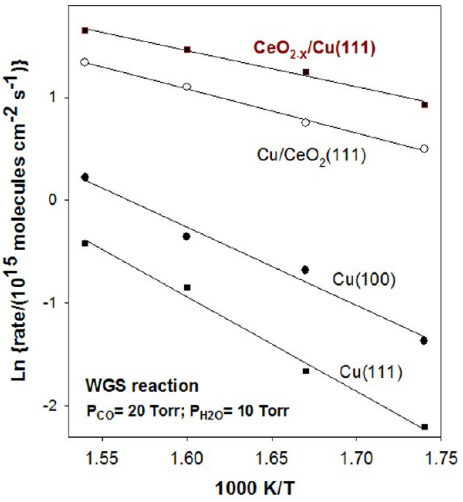

FIGURE 7. Arrhenius plot of Cu based catalysts including Cu(111), Cu(100), $Cu/CeO_2(111)$, and $CeO_{2-x}/Cu(111)$. $P_{CO} = 20$ Torr; $P_{H_2O} = 10$ Torr; $T = 575$, 600, 625, and 650 K. Reprinted with permission from ref 11. Copyright 2009 Wiley and Sons.

oxide nanoparticle are unique, and the interaction with the Cu substrate, in particular the interface, is very important to lowering the barrier to H_2O dissociation and the subsequent reaction with CO that leads to the production of H_2.[11] Post mortem XPS analysis of the inverse catalyst showed that the oxide nanoparticles were rich in Ce^{3+} while the support was Cu^0. This is different from the supported catalyst where there Ce^{3+} was only a minority component in the post mortem analysis and potentially explains the difference in activity due to the simple fact that ceria "3+" sites remain exposed to the stream of reactants while in the supported catalyst remain occupied by metal particles. Many of the features observed for the WGS on a model $CeO_2/Cu_2O/Cu(111)$ catalyst has also been observed for powder CeO_2/CuO catalysts.[13] In both systems the copper oxide is fully reduced while a large amount of Ce^{3+} is formed under reaction conditions. This Ce^{3+} is directly involved in the dissociation of water.[11,13]

b. CO Oxidation. Remediation of carbon monoxide, a commonly found noxious gas, is important to several technological areas including automotive exhausts catalysis that seeks to limit pollutant emissions; fuel cell applications where CO tends to poison PEM catalysts; and synthesis gas conversion where the CO preferential oxidation reaction (PROX) usually follows the WGS to remove any residual CO. In these processes, the easiest way to remove CO is to convert it to CO_2 through oxidation with O_2 ($2CO + O_2 \rightarrow 2CO_2$). CuO_x and copper-oxide-based catalysts have shown great promise toward this reaction and often are the standard for regular and H_2 rich (PROX) reactions. In fact, high surface area powder catalysts with an inverse CeO_2/CuO configuration have demonstrated superior performance for the oxidation of CO.[12]

$$O_2(g) \rightarrow O_2(a)$$

$$CO(g) \rightarrow CO(a)$$

$$O_2(a) \rightarrow O(a) + O(a)$$

$$CO(a) + O(a) \rightarrow CO_2(a)$$

$$CO_2(a) \rightarrow CO_2(g)$$

The role of the Ceria nanoparticles and the Cu support in this inverse configuration was challenging to understand. An inverse model catalysts composed of $CeO_2/Cu_2O/Cu(111)$ was used to study this process in a systematic and fundamental way.[28]

Catalytic testing was performed with these model systems using a batch reactor with CO (20 Torr) and O_2 (10 Torr) at a range of temperatures from 550 to 700 K. These results showed that the presence of ceria nanoparticles on the Cu(111) substrate improved considerably the activity with respect to the Cu(111) substrate alone (Figure 8). In a set of experiments, the combination of XPS and STM established that the supported ceria nanoparticles were quite efficient for adsorbing and dissociating the O_2 molecule, with a subsequent spilling of O to the copper substrate and an enhancement in the rate of CuO_x formation.[28] DFT calculations for these inverse catalysts corroborated the importance of the role of the ceria nanoparticles.[28] They identified that ceria nanoparticles in the oxide/metal configuration had special electronic properties clearly evident in the DOS of the system. These electronic properties provided good stability to supported ceria and at the same time enough activity to dissociate O_2. Furthermore, the O deposited on the ceria by dissociation of O_2 could be removed by direct reaction with CO. In Figure 9, the reduction with CO in all cases is much more favored than the oxidation with O_2. This makes possible the closure of a catalytic cycle for CO oxidation. Due to their special electronic and chemical properties, the supported ceria nanoparticles alone could catalyze the oxidation of CO. However, in the actual process, one could have interaction of adsorbed CO with oxygen directly on top of ceria or on the copper substrate after spillover of the oxygen. The place of reaction will be determined by the rate of adsorption of CO on ceria, copper oxide, or the interface of the oxides. Thus, the configuration of the inverse oxide/metal catalyst opens new interesting routes for applications in catalysis.

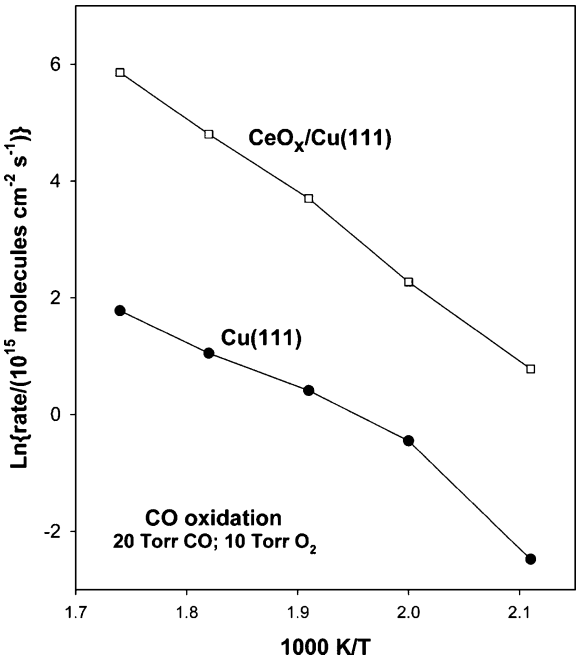

FIGURE 8. Arrhenius plot of Cu based catalysts including Cu(111), and CeO_{2-x}/Cu(111) at CO (20 Torr) + O_2 (10 Torr).

It was found that the CeO_2/Cu_2O/Cu(111) catalysts have activities for the $2CO + O_2 \rightarrow 2CO_2$ reaction that are comparable or larger than those reported for surfaces of expensive noble metals such as Rh(111), Pd(110), and Pt(100).[28] CeO_x nanoparticles also can be added to noble-metal surfaces to enhance their activity for CO oxidation,[45,46] but these systems are not as active and seem to behave in a different way with respect to the CeO_2/Cu_2O/Cu(111) system where ceria is very efficient for the dissociation of O_2 and accelerates the oxidation of the copper substrate.

5. Ceria Nanoparticles and Surface Reconstructions

One of the major goals of catalysis research is the understanding of structural and surface changes induced by the presence of adsorbates.[47] Having the ability to control or influence surface changes is important to ultimately drive reactions toward designed products. However, the behavior of metals, oxides and the effect of oxides on these catalyst surfaces during a reaction remain relatively unexplored; controlling adsorbate induced changes remains challenging. Reconstructions or transformations of a metal surface can lead to changes in the steps of a catalytic process as a result of structural and electronic effects. On one hand, different surface geometries can provide different sites for molecules to bond. And on the other hand, a difference in electronic properties can produce a change in the way in which electrons localized

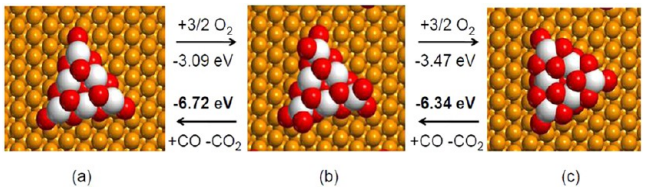

FIGURE 9. Top view of the optimized structures of the particles (a) Ce_6O_{13}, (b) Ce_6O_{16}, and (c) Ce_6O_{19}. The energies involved in the interconversion by oxidative–reductive cycles with O_2 or CO are shown. Atom colors: Ce (white), O (soft-red), and Cu (golden). Reprinted with permission from ref 28. Copyright 2011 American Chemical Society.

in active sites respond to reactants. Cu(111) surfaces have never been reported to undergo surface reconstructions upon contact with a reactant such as O_2, however higher index surfaces such as Cu(115) and Cu(119) facet upon contact with oxygen.[48]

Our structural studies of the inverse catalysts have led us to discover a unique relationship between the CeO_x nanoparticles and the Cu(111) substrate.[49] During the preparation of CeO_x nanoparticles, a deep oxidation of the Cu(111) surface can occur that takes the oxide layer from Cu_2O to CuO_{1-x} through a mechanism that involves the dissociation of O_2 on ceria sites and spillover of O onto the Cu substrate as discussed in the previous section.[28] This CeO_x/CuO_{1-x} surface when heavily reduced using CO (5×10^{-7} Torr, 600 K), which is the typical reducing agent found in both the WGS and the CO oxidation reactions, leaves the Cu(111) substrate with a massive surface reconstruction as depicted using LEEM in Figure 10 below. CO attacks all components of the inverse CeO_2/CuO_{1-x}/Cu(111) catalyst removing O ($CO + O \rightarrow CO_2$) from both the CeO_2 ($Ce^{4+} \rightarrow Ce^{3+}$) and the CuO_{1-x}($Cu^{2+} \rightarrow Cu^{1+} \rightarrow Cu^0$), but in particular moves the Cu atoms to form microterraces that cover 25–35% of the surface.[48] This process depends exclusively on the CeO_x nanoparticles and the preoxidation process and is not observed on either Cu_2O/Cu(111) or the as grown CeO_x/Cu(111) surface upon reduction with CO under similar conditions.

When one compares the WGS activity of this massively reconstructed (mr) surface to that of the as grown (reg) CeO_x/Cu(111) surface (Arrhenius plot in Figure 10), it is evident that the reconstruction can lead to an increase in H_2 production and the rate of the WGS reaction. In a relative comparison of the Cu(111) and CeO_x/Cu(111)-mr surfaces, one finds that the activation energy decreases from 18 to 7 kcal/mol.[49] As discussed above, studies for the as grown CeO_x/Cu(111) surface showed that the presence of CeO_x nanoparticles aids in the dissociation of H_2O, a step that was difficult for Cu(111), and contributes to the high WGS activity of the

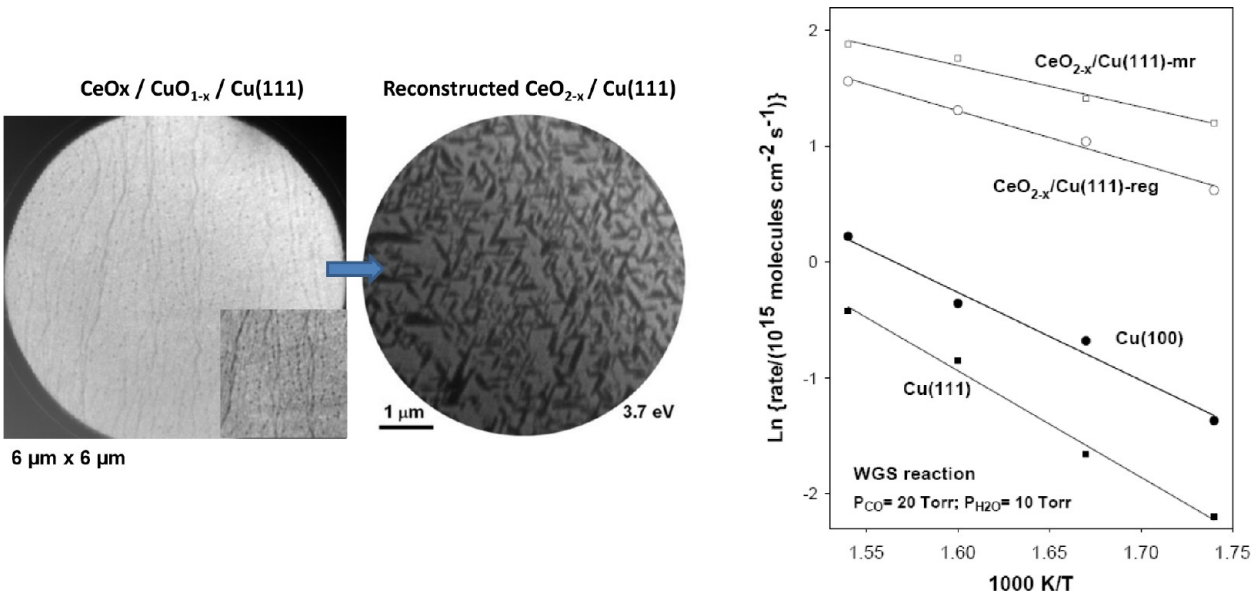

FIGURE 10. Left: LEEM images of as grown (left) and reconstructed CeO_x nanoparticles on Cu(111) substrate (right). Right: Arrhenius plot of Cu based catalysts including Cu(111), and CeO_{2-x}/Cu(111) at CO (20Torr) + O_2 (10Torr). Reprinted with permission from ref 49. Copyright 2012 American Chemical Society.

inverse catalyst. However, in this instance, the reconstructed surface goes further with its Cu microterraces likely involved in further enhancing the rate of H_2O dissociation. Indeed, postreaction characterization with XPS showed a much higher abundance of Cu−OH species on the reconstructed surface than on the unreconstructed CeO_x/Cu surface. XPS proved that remarkably the dissociation of water was occurring in two paths on the reconstructed surface: over the CeO_x nanoparticles and over the Cu sites on the microterraces.[48] These active sites were then able to yield an enhancement in activity for the WGS reaction. The data in Figure 10 illustrate the tremendous effects that oxide nanoparticles can have on the structural and chemical properties of metal surfaces.

6. Conclusions

Inverse model catalysts are an ideal test bed for studying catalytic processes. These models provide a unique opportunity to undertake fundamental investigations into the structure, active components, and mechanistic pathways using experimental (STM, XPS, LEEM) and theoretical (DFT) tools. In the previous sections, we have focused on studies for the deposition of ceria nanoparticles on Cu_2O/Cu(111) or Cu(111). Similar studies also could be performed for systems involving nanoparticles of ceria dispersed on Ni,[30] Rh,[32] Ru,[33,34] Pd,[35] Re,[36] Pt,[37,38] and Au.[5] Furthermore, instead of using ceria, one could deposit nanoparticles of titania[5,6] or iron oxide[50−52] on top of a metal surface. Thus, in the future, other inverse systems similar to the CeO_x/Cu(111) model but composed of different oxide/metal combinations will be able to provide insights into structure−reactivity relationships while identifying key components that drive catalytic reactions aimed toward selective chemical products. In an inverse oxide/metal catalyst, one takes advantage of the special properties that oxide nanoparticles have. These special properties can be useful for fundamental studies, as shown above, or for the preparation of highly active high-surface area powders.[12,13]

The work performed at BNL was supported by the U.S. Department of Energy, Office of Basic Energy Sciences, under Contract DE-AC02-98CH10886. Part of these studies was done at the National Synchrotron Light Source and at the Center for Functional Nanomaterials of BNL, which are supported by the U.S. Department of Energy.

BIOGRAPHICAL INFORMATION

Sanjaya D. Senanayake received his B.Tech. (Materials) with Hons in 2001 and Ph.D. in Chemistry in 2006 from The University of Auckland in New Zealand. After postdoctoral work with Oak Ridge National Lab and Brookhaven National Laboratory, he is at present an Assistant Scientist in the Department of Chemistry at Brookhaven National Laboratory. He also serves as the beamline scientist at X7B at the National Synchrotron Light Source.

Dario Stacchiola is an Associate Chemist at Brookhaven National Laboratory and Adjunct Professor at Michigan Technological University. He obtained his B.S. degree (1997) at UNSL (Argentina), Ph.D. (2002) at the University of Wisconsin—Milwaukee, and was a Humboldt Research Fellow at the Fritz-Haber-Institute in Berlin (2005−2007). His research interest is in Surface Chemistry, in particular on the structure−reactivity relationships in Catalysis.

Jose A. Rodriguez did part of his education at Simon Bolivar University in Venezuela, where he received B.S. degrees in Chemistry and Chemical Engineering, and a M.S. in Theoretical Chemistry. He moved to the United States to get a Ph.D. in Physical Chemistry at Indiana University, Bloomington. He is currently a Senior Scientist at Brookhaven National Laboratory and an Adjunct Professor in the Department of Chemistry of SUNY Stony Brook. Nowadays, Dr. Rodriguez is involved in the preparation and study of nanocatalyts utilized for the production of clean fuels and the control of environmental pollution.

FOOTNOTES

*To whom correspondence should be addressed. E-mail: rodrigez@bnl.gov. Fax: 1-631-344-5815.

The authors declare no competing financial interest.

REFERENCES

1 Cox, P. A. *Transition Metal Oxides: An Introduction to Their Electronic Structure and Properties*; Oxford University Press: Oxford, U.K., 2010; pp 1−294.

2 Jackson, S. D.; Hargreaves, J. S. J.*Metal Oxide Catalysis*; Wiley-VCH: New York, 2008; pp 1−887.

3 Noguera, C. *Physics and Chemistry at Oxide Surfaces*; Cambridge University Press: Cambridge, U.K., 2005; pp 1−240.

4 Wu, J.; Cao, J.; Han, W.-Q.; Janotti, A.; Kim, H.-C. *Functional Metal Oxide Nanostructures*; Springer: Berlin, 2012; pp 1−379.

5 Rodriguez, J.; Ma, S.; Liu, P.; Hrbek, J.; Evans, J.; Perez, M. Activity of CeO_x and TiO_x nanoparticles grown on Au(111) in the water-gas shift reaction. *Science* **2007**, *318*, 1757–1760.

6 Fujitani, T.; Nakamura, I. Mechanism and active sites of the oxidation of CO over Au/TiO_2. *Angew. Chem., Int. Ed.* **2011**, *50*, 10144–10147.

7 Sun, Y.; Qin, Z.; Lewandowski, M.; Carrasco, E.; Sterrer, M.; Shaikhutdinov, S.; Freund, H. Monolayer iron oxide film on platinum promotes low temperature CO oxidation. *J. Catal.* **2009**, *266*, 359–368.

8 Demmin, R.; Ko, C.; Gorte, R. Effect of titania on the chemisorption and reaction properties of Pt. *J. Phys. Chem.* **1985**, *89*, 1151–1154.

9 Castellarin-Cudia, C.; Surnev, S.; Schneider, G.; Podlucky, R.; Ramsey, M.; Netzer, F. Strain-induced formation of arrays of catalytically active sites at the metal-oxide interface. *Surf. Sci.* **2004**, *554*, L120–L126.

10 Rodriguez, J.; Hrbek, J. Inverse oxide/metal catalysts: A versatile approach for activity tests and mechanistic studies. *Surf. Sci.* **2010**, *604*, 241–244.

11 Rodriguez, J.; Graciani, J.; Evans, J.; Park, J.; Yang, F.; Stacchiola, D.; Senanayake, S.; Ma, S.; Perez, M.; Liu, P.; Sanz, J.; Hrbek, J. Water-Gas shift reaction on a highly active inverse $CeO_x/Cu(111)$ catalyst: Unique role of ceria nanoparticles. *Angew. Chem., Int. Ed.* **2009**, *48*, 8047–8050.

12 Hornes, A.; Hungria, A.; Bera, P.; Camara, A.; Fernandez-Garcia, M.; Martinez-Arias, A.; Barrio, L.; Estrella, M.; Zhou, G.; Fonseca, J.; Hanson, J.; Rodriguez, J. Inverse CeO_2/CuO catalyst as an alternative to classical direct configurations for preferential oxidation of CO in hydrogen-rich stream. *J. Am. Chem. Soc.* **2010**, *132*, 34–35.

13 Barrio, L.; Estrella, M.; Zhou, G.; Wen, W.; Hanson, J.; Hungria, A.; Hornes, A.; Fernandez-Garcia, M.; Martinez-Arias, A.; Rodriguez, J. Unraveling the active site in copper-ceria systems for the Water-Gas shift reaction: In situ characterization of an inverse powder CeO_{2-x}/CuO-Cu Catalyst. *J. Phys. Chem. C* **2010**, *114*, 3580–3587.

14 Trovarelli, A. Catalytic properties of ceria and CeO_2-containing materials. *Catal. Rev.: Sci. Eng.* **1996**, *38*, 439–520.

15 Fernandez-Garcia, M.; Martinez-Arias, A.; Hanson, J.; Rodriguez, J. Nanostructured oxides in chemistry: Characterization and properties. *Chem. Rev.* **2004**, *104*, 4063–4104.

16 Zhang, F.; Chan, S.; Spanier, J.; Apak, E.; Jin, Q.; Robinson, R.; Herman, I. Cerium oxide nanoparticles: Size-selective formation and structure analysis. *Appl. Phys. Lett.* **2002**, *80*, 127–129.

17 Wang, Z.; Feng, X. Polyhedral shapes of CeO_2 nanoparticles. *J. Phys. Chem. B* **2003**, *107*, 13563–13566.

18 Sayle, T.; Parker, S.; Sayle, D. Shape of CeO_2 nanoparticles using simulated amorphisation and recrystallisation. *Chem. Commun.* **2004**, 2438–2439.

19 Cordatos, H.; Ford, D.; Gorte, R. Simulated annealing study of the structure and reducibility in ceria clusters. *J. Phys. Chem.* **1996**, *100*, 18128–18132.

20 Zhou, G.; Shah, P. R.; Montini, T.; Fornasiero, P.; Gorte, R. J. Oxidation enthalpies for reduction of ceria surfaces. *Surf. Sci.* **2007**, *601*, 2512–2519.

21 Loschen, C.; Bromley, S.; Neyman, K.; Illas, F. Understanding ceria nanoparticles from first-principles calculations. *J. Phys. Chem. C* **2007**, *111*, 10142–10145.

22 Loschen, C.; Migani, A.; Bromley, S.; Illas, F.; Neyman, K. Density functional studies of model cerium oxide nanoparticles. *Phys. Chem. Chem. Phys.* **2008**, *10*, 5730–5738.

23 Bromley, S.; Moreira, I.; Neyman, K.; Illas, F. Approaching nanoscale oxides: models and theoretical methods. *Chem. Soc. Rev.* **2009**, *38*, 2657–2670.

24 Vayssilov, G.; Mihaylov, M., St; Petkov, P.; Hadjiivanov, K.; Neyman, K. Reassignment of the vibrational spectra of carbonates, formates, and related surface species on ceria: A combined density functional and infrared spectroscopy investigation. *J. Phys. Chem. C* **2011**, *115*, 23435–23454.

25 Sadowski, J. T.; Senanayake, S. D.; Flege, J. T.; Kaema, B. In preparation.

26 Yang, F.; Choi, Y.; Liu, P.; Stacchiola, D.; Hrbek, J.; Rodriguez, J. Identification of 5−7 defects in a copper oxide surface. *J. Am. Chem. Soc.* **2011**, *133*, 11474–11477.

27 Jensen, F.; Besenbacher, F.; Laegsgaard, E.; Stensgaard, I. Oxidation of Cu(111) - 2 new oxygen induced reconstructions. *Surf. Sci.* **1991**, *259*, L774–L780.

28 Yang, F.; Graciani, J.; Evans, J.; Liu, P.; Hrbek, J.; Frd-Sanz, J.; Rodriguez, J. CO oxidation on inverse $CeO_x/Cu(111)$ catalysts: High catalytic activity and ceria-promoted dissociation of O-2. *J. Am. Chem. Soc.* **2011**, *133*, 3444–3451.

29 Yang, F.; Choi, Y.; Agnoli, S.; Liu, P.; Stacchiola, D.; Hrbek, J.; Rodriguez, J. CeO_2 <-> CuO_x interactions and the controlled assembly of $CeO_2(111)$ and $CeO_2(100)$ nanoparticles on an oxidized Cu(111) substrate. *J. Phys. Chem. C* **2011**, *115*, 23062–23066.

30 Mullins, D.; Radulovic, P.; Overbury, S. Ordered cerium oxide thin films grown on Ru(0001) and Ni(111). *Surf. Sci.* **1999**, *429*, 186–198.

31 Matolin, V.; Sedlacek, L.; Matolinova, I.; Sutara, F.; Skala, T.; Smid, B.; Libra, J.; Nehasil, V.; Prince, K. Photoemission spectroscopy study of Cu/CeO_2 systems: Cu/CeO_2 nanosized catalyst and $CeO_2(111)$/CU(111) inverse model catalyst. *J. Phys. Chem. C* **2008**, *112*, 3751–3758.

32 Castellarin-Cudia, C.; Surnev, S.; Schneider, G.; Podlucky, R.; Ramsey, M.; Netzer, F. Strain-induced formation of arrays of catalytically active sites at the metal-oxide interface. *Surf. Sci.* **2004**, *554*, L120–L126.

33 Mullins, D.; Robbins, M.; Zhou, J. Adsorption and reaction of methanol on thin-film cerium oxide. *Surf. Sci.* **2006**, *600*, 1547–1558.

34 Lu, J.; Gao, H.; Shaikhutdinov, S.; Freund, H. Morphology and defect structure of the $CeO_2(111)$ films grown on Ru(0001) as studied by scanning tunneling microscopy. *Surf. Sci.* **2006**, *600*, 5004–5010.

35 Alexandrou, M.; Nix, R. The growth, structure and stability of ceria overlayers on Pd(111). *Surf. Sci.* **1994**, *321*, 47–57.

36 Xiao, W.; Guo, Q.; Wang, E. Transformation of $CeO_2(111)$ to $Ce_2O_3(0001)$ films. *Chem. Phys. Lett.* **2003**, *368*, 527–531.

37 Berner, U.; Schierbaum, K. Cerium oxides and cerium-platinum surface alloys on Pt(111) single-crystal surfaces studied by scanning tunneling microscopy. *Phys. Rev. B* **2002**, *65*, 235404.

38 Berner, U.; Schierbaum, K.; Jones, G.; Wincott, P.; Haq, S.; Thornton, G. Ultrathin ordered CeO_2 overlayers on Pt(111): interaction with NO_2, NO, H_2O and CO. *Surf. Sci.* **2000**, *467*, 201–213.

39 Nakamura, J.; Campbell, J.; Campbell, C. Kinetics and mechanism of the water-gas shift reaction catalyzed by the clean and Cs-promoted Cu(110) surface − a comparison with Cu(111). *J. Chem. Soc., Faraday Trans.* **1990**, *86*, 2725–2734. Campbell, C.; Daube, K. A surface science investigation of the water-gas shift reaction on Cu(111). *J. Catal.* **1987**, *104*, 109–119.

40 Jernigan, G.; Somorjai, G. Carbon-monoxide oxidation over 3 different oxidation-states of copper − metallic copper, copper (I) oxide, and copper (II) oxide − a surface science and kinetic study. *J. Catal.* **1994**, *147*, 567–577.

41 Gokhale, A.; Dumesic, J.; Mavrikakis, M. On the mechanism of low-temperature water gas shift reaction on copper. *J. Am. Chem. Soc.* **2008**, *130*, 1402–1414.

42 Zhang, C.; Baxter, R.; Hu, P.; Alavi, A.; Lee, M. A density functional theory study of carbon monoxide oxidation on the $Cu_3Pt(111)$ alloy surface: Comparison with the reactions on Pt(111) and Cu(111). *J. Chem. Phys.* **2001**, *115*, 5272–5277.

43 Ratnasamy, C.; Wagner, J. Water-Gas shift catalysis. *Catal. Rev.: Sci. Eng.* **2009**, *51*, 325–440.

44 Jakdetchai, O.; Nakajima, T. Mechanism of the water-gas shift reaction over Cu(110), Cu(111) and Cu(100) surfaces: an AM1-d study. *J. Mol. Struct.: THEOCHEM* **2002**, *619*, 51–58.

45 Suchorski, Y.; Wrobel, R.; Becker, S.; Weiss, H. CO oxidation on a $CeO_x/Pt(111)$ inverse model catalyst surface: Catalytic promotion and tuning of kinetic phase diagrams. *J. Phys. Chem. C* **2008**, *112*, 20012–20017.

46 Eck, S.; Castellarin-Cudia, C.; Surnev, S.; Prince, K.; Ramsey, M.; Netzer, F. Adsorption and reaction of CO on a ceria-Rh(111) ″inverse model catalyst″ surface. *Surf. Sci.* **2003**, *536*, 166–176.

47 Tao, F.; Dag, S.; Wang, L.; Liu, Z.; Butcher, D.; Bluhm, H.; Salmeron, M.; Somorjai, G. Break-up of stepped platinum catalyst surfaces by high CO coverage. *Science* **2010**, *327*, 850–853.

48 Reinecke, N.; Taglauer, E. The kinetics of oxygen-induced faceting of Cu(115) and Cu(119) surfaces. *Surf. Sci.* **2000**, *454*, 94–100.

49 Senanayake, S.; Sadowski, J.; Evans, J.; Kundu, S.; Agnoli, S.; Yang, F.; Stacchiola, D.; Flege, J.; Hrbek, J.; Rodriguez, J. Nanopattering in CeO_x/Cu(111): A new type of surface reconstruction and enhancement of catalytic activity. *J. Phys. Chem. Lett.* **2012**, *3*, 839–843.

50 Sun, D.; Gu, X.; Ouyang, R.; Su, H.; Fu, Q.; Bao, X.; Li, W. Theoretical study of the role of a metal-cation ensemble at the oxide-metal boundary on CO oxidation. *J. Phys. Chem. C* **2012**, *116*, 7491–7498.

51 Sun, Y.; Qin, Z.; Lewandowski, M.; Carrasco, E.; Sterrer, M.; Shaikhutdinov, S.; Freund, H. Monolayer iron oxide film on platinum promotes low temperature CO oxidation. *J. Catal.* **2009**, *266*, 359–368.

52 Yan, T.; Redman, D. W.; Yu, W.-Y.; Flaherty, D. W.; Rodriguez, J. A.; Mullins, C. B. CO oxidation on inverse Fe_2O_3/Au(111) model catalysts. *J. Catal.* **2012**, *294*, 216–228.